CLAWAR 2020: 23rd International Conference on
Climbing and Walking Robots and the Support
Technologies for Mobile Machines,
Moscow, Russian Federation, 24-26 August 2020.
https://doi.org/10.13180/clawar.2020.24-26.08.40

DEVELOPMENT OF METHODS FOR AUTOMATIC CONTROL OF MANIPULATOR DRIVES OF MOBILE WEEDING ROBOT WITH PARALLEL-SERIAL STRUCTURE

A. G. IVANOV and N. S. VOROB'YEVA

Volgograd State Agrarian University,
Volgograd, University Avenue 26, 400002, Russia;
E-mail: leha_2106@list.ru, vgsxa@mail.ru
http://www.volgau.com/

V. V. ZHOGA

Volgograd State Technical University,
Volgograd, Lenin Avenue 28, 400005, Russia;
Center for Technologies in Robotics and Mechatronics Components, Innopolis University,
Innopolis, Universitetskaya Str. 1, 420500, Russia;
E-mail: viczhoga@gmail.com

V. E. PAVLOVSKY and E. V. PAVLOVSKY

Keldysh Institute of Applied Mathematics (Russian Academy of Sciences),
Moscow, Miusskaya sq. 4, 125047, Russia.
E-mail: vlpavl@mail.ru

Abstract. The work solved the problem of positioning - determining the lengths of the actuating links of the manipulator with a parallel-serial structure at a given position of the operating body. A kinematic algorithm for manipulator position stabilization in a given final state is synthesized. A mathematical model of the spatial controlled motion dynamics of the operating body as a multi-mass system is developed. The control efforts change laws are obtained.

The article considers the development of a control algorithm for the actuating links of a manipulator with a parallel-serial structure. The authors suggest a two-stage procedure for resolving the problem of controlling the robot operating body motion into a set neighborhood of the final state for a set time. The first stage covers the process of solving the problem of defining the manipulator generalized coordinates at the set coordinates of the operating body. The problem solution is of an optimization nature. The second stage proceeds with the resolving of the problem of defining the laws of the setting action formation for the actuating drives responsible for the operating body motion in the set point neighborhood. The programmed path correction is done in such a way that at any specific time it moves through a set position of the operating body while the deviations from the final state of actuating links change according to the solution of the formed differential equation. The authors develop a mathematical model for the dynamics of the operating body motion taking into account it is a multi-mass system. The article provides the obtained laws regulating changes in control forces. Finally, the authors give the results of computational modeling to prove the algorithm practical efficiency by the example of a specific manipulator.

Key words: weeding robot, manipulator with a parallel-spatial structure, positioning, control system, mathematical model of dynamics.

When cultivating vegetables and cucurbits, one of the time-consuming and energy-consuming tillage operations is weeding, commonly carried out by cultivation. The effectiveness of mechanical weed control largely depends on the weeding quality. Manual weeding is still practiced for raising vegetables and cucurbits in open ground. This is also explained by the fact that in case of the mechanical destruction of weeds the operating bodies of the cultivator (“arms”) process only the aisles. To solve the problem of complete weeding, both in row spacings and in rows, a weeding robot was developed (Figure 1) for the target weeding.

The weeding robot consists of a frame 1, steered wheels 2, a control and navigation system with instrumentation 3, a power supply system 4 and a computer vision sensor 7 [1].

The motion mechanism of the operating body of the weeding robot (Figure 2) is a flat mechanism of a parallel-serial structure with three degrees of freedom [2]. To move the operating body 8 in the horizontal plane, three linear actuators 5 are used, and the linear actuator 6 is used to move the operating body in a vertical plane. The operating body is rotated by means of the electric motor 9.

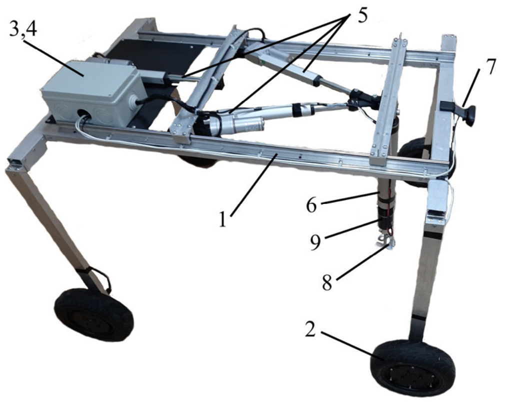

Figure 1. Mobile weeding robot.

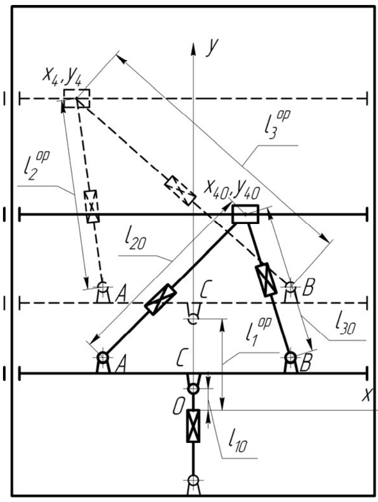

Figure 2. The design model of the mechanism for moving the operating body of the weeding robot. Top view

With the help of the control and navigation system, the weeding robot drives into the plant beds. In the automatic mode, using the computer vision sensor, the coordinates of the location of weeds in a row are obtained. The cutting tool of the operating body moves to the weed. When the cutting tool of the operating body is above the weed, the linear actuator moves the operating body vertically down to cut the weed and loosen the soil next to it.

1. Problem statement

For the implementation of the described technology, it is necessary to develop algorithms for the formation of a system to control the motion of the weeding robot operating body. The control system must set the motion of the operating body to a given point in the operating area with a required accuracy. The motion of the manipulator in the horizontal plane is considered. The generalized manipulator coordinates are the lengths of the actuating links $q_1 = l_1(t), \quad q_2 = l_2(t), \quad q_3 = l_3(t)$. The motion of the operating body from a known initial position with coordinates (x_{40}, y_{40}) to a predetermined final position (x_4, y_4) is provided by changing the lengths $l_i(t), \ (i = 1 \div 3)$ of the manipulator actuating links. The problem is solved in two stages. First, the positioning problem is solved: for the given final coordinates (x_4, y_4) of the attachment point of the vertical actuator (Figure 2), it is required to obtain the generalized coordinates of the manipulator $l_i^{op}, \ (i = 1 \div 3)$. Since the number of the Cartesian coordinates of the actuator attachment point is two, and the number of generalized coordinates of the manipulator is three, the maneuverability of the manipulator is one [3]. That is, the final position of the actuator with the operating body corresponds to an infinite number of manipulator configurations. Thus, the solution of this problem is of an optimization nature.

At the second stage, it is necessary to define the laws of change in the generalized coordinates of the manipulator $l_i(t),\ (i=1\div3)$, when moving the attachment point of the operating body from the initial one to the neighborhood of the designated point. As control parameters take the acceleration of changes in the generalized coordinates $\ddot{l}_i(t),\ (i=1\div3)$.

2. Solution methods

Manipulator positioning. The design of the manipulator stipulates for the holonomic constraints between the coordinates of the point $O_4(x_4, y_4)$, the lengths of the actuating links and the manipulator geometric parameters

$$l_2 = \sqrt{\left(y_4 - l_1\right)^2 + \left(AC + x_4\right)^2}, \quad l_3 = \sqrt{\left(y_4 - l_1\right)^2 + \left(BC - x_4\right)^2} \tag{1}$$

The configuration of the manipulator is determined from the minimum condition of the quadratic function - the criterion of generalized energy [4]

$$\Phi = \sum_{i=1}^{3} c_i \cdot (l_{ik} - l_{i0})^2$$

with inequality constraints

$$l_{i\min} \le l_i^{op} \le l_{i\max}, \tag{2}$$

where c_1, c_2, c_3 are weighting factors, the values of which are proportional to the loads on the actuating links; $l_{i\min}, l_{i\max}$ are the minimum and maximum permissible values of the lengths of the manipulator actuating links (Figure 2); l_i^{op} is an optimal length.

The Lagrange objective function has the form [5]

$$\Phi^* = \sum_{i=1}^{3} c_i (l_{ik} - l_{i0})^2 + \lambda_{2i-1}\left(u_{2i-1}^2 + l_i - l_{2i-1,\max}\right) + \lambda_{2i}\left(u_{2i}^2 + l_{i\min} - l_i\right), \tag{3}$$

where u_i^2 are auxiliary functions; λ_i are Lagrange multipliers.

The necessary conditions for the extremum of function (3) are written in the form

$$\frac{\partial \Phi^*}{\partial l_1} = c_1 \frac{\partial (l_{1i} - l_{10})^2}{\partial l_1} + c_2 \frac{\partial (l_{2i} - l_{20})^2}{\partial l_1} + c_3 \frac{\partial (l_{3i} - l_{30})^2}{\partial l_1} + \lambda_1 - \lambda_2 = 0, \tag{4}$$

$$\begin{aligned} &\lambda_{2i-1} = 0,\ if,\ l_i^{op} < l_{imax};\ \lambda_{2i} = 0,\ if,\ l_i^{op} > l_{imin}, \\ &\lambda_{2i-1} > 0,\ if,\ l_i^{op} = l_{imax};\ \lambda_{2i} > 0,\ if,\ l_i^{op} = l_{imin} \end{aligned} \tag{5}$$

Since the Lagrange function (3) is convex, and the multipliers $\lambda_{2i-1} \ge 0,\ \lambda_{2i} \ge 0$, the necessary conditions (4), (5) are sufficient.

Stabilization of the manipulator given position. Since the manipulator has great rigidity, the Cartesian coordinates of the actuator attachment points with the operating body are determined through the lengths of the actuating links with a high accuracy [6]

$$x_4 = \frac{l_3^2 - l_2^2}{4AC}, \quad y_4 = l_1 + \sqrt{l_2^2 - \left(\frac{l_3^2 - l_2^2}{4AC}\right)^2 + \frac{l_3^2 - l_2^2}{2} - AC^2}. \tag{6}$$

The requirements for control accuracy are set only to the end point, without imposing restrictions on the path of the characteristic point, which may change during the motion of the operating body due to external disturbances. Assume that for each actuating link control loops are known; they are closed by generalized coordinates $l_i(t),\ i=1\div 3$ [7]. In this case, the solution of the problem is reduced to determining the laws of formation of the setting actions $l_i(t)$ for the executive drives, ensuring the motion of the operating body in the neighborhood of a given point on the plane to which the lengths of the actuating links $l_i(\tau)=\ l_i^{op}$, $i=1\div 3$ correspond. Assume that on the motion path the deviations from the final state of the actuating links $\Delta l_i(t)=l_i^{op}-l_i(t)$ change in accordance with the solution of the differential equation

$$\Delta\ddot{l}_i(t)+a_{1i}\Delta\dot{l}_i(t)+a_{2i}\Delta l_i(t)=0\,, \tag{7}$$

where a_{1i}, a_{2i} are constant positive numbers.

The following differential equations correspond to the laws of the formation of the setting actions $l_k(t)$ of the actuators determined by equations (7)

$$\ddot{l}_i(t)+a_{i1}\dot{l}_i(t)+a_{i2}l_i(t)=a_{i2}l_i^{op}\,, \tag{8}$$

under the initial conditions describing the manipulator state at $t_0=0$

$$l_i(0)=l_{i0},\quad \dot{l}_i(0)=\dot{l}_{i0}. \tag{9}$$

A general solution for the equation (8) is a total of a general solution for the homogeneous equation and a partial solution of a heterogeneous equation; it has the form

$$l_i(t)=C_{1i}e^{p_{1i}t}+C_{2i}e^{p_{2i}t}+l_i^{op} \tag{10}$$

where the roots p_{1i}, p_{2i} are the roots of the corresponding characteristic homogeneous equation.

The integration constants are obtained from (8), taking into account (9)

$$C_{1i}=\frac{\Delta l_i(0)p_{2i}+\dot{l}_{i0}}{\left(p_{1i}-p_{2i}\right)},\quad C_{2k}=-\frac{\Delta l_i(0)p_{1i}+\dot{l}_{i0}}{\left(p_{1i}-p_{2i}\right)},\quad \Delta l_i(0)=l_i^{op}-l_i(0)\quad , \tag{11}$$

The coefficients of equations (8) are determined using the roots of the characteristic equation

$$a_{1i}=-\left(p_{1i}+p_{2i}\right),\ a_{2i}=p_{1i}p_{2i}$$

To satisfy the requirement $l_i(t)\to l_i^{op}$ for $t\to\infty$, the difference of the characteristic equation roots is negative.

The law of changing the lengths of the actuating links (10) is programmed. To construct a feedback control law, it is necessary to calculate the required acceleration from the current values of the generalized coordinates

$$\ddot{l}_i(t)=a_{i2}l_i^{op}-a_{i1}\dot{l}_i(t)-a_{i2}l_i(t)\,, \tag{12}$$

Thus, in the expressions (11), it is necessary to consider the current values of the generalized coordinates as initial. The feedback in the drive motor control loops is obtained by the variables

$l_i(t), \dot{l}_i(t)$. The values of these variables are used for calculating the expressions included in the equation (12). Figure 3 shows a control system structural diagram.

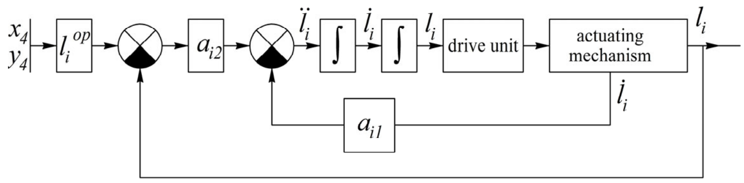

Figure 3. Control system structural diagram

3. Control system structure

The main architectural features of the control system are defined by the robot mechanical structure, the nature of the programmed motions and the range of tasks to be resolved.

Functionally, the control system can be divided into two levels. The upper level provides general motion planning, GPS receiver data processing and navigation, communication with the remote control and telemetry via Wi-Fi protocol, implements a computer vision system.

The top level is based on the Raspberry Pi 3 Model B microcomputer. This microcomputer is based on the Broadcom BCM2837 processor with four 64-bit ARM Cortex A-53 cores operating at 1.2 GHz, has 1 GB of RAM, USB, RS-232, I2C and GPIO ports, an integrated Wi-Fi unit. The use of a full-fledged microcomputer in the control system instead of the microcontroller allows the implementation of fairly complex control algorithms, WiFi support and the construction of a computer vision system.

The lower level of the control system directly controls the actuating mechanisms of the weeding robot.

3.1. Actuating Mechanism Control

The actuating mechanisms, or actuators, of the weeding robot are divided into two groups (Figure 4). The first consists of linear actuators (SKF CAHB-21-B1N-610926-AAA0P0-000) used in the construction of the manipulator, and the second includes servomotors for robot horizontal motion.

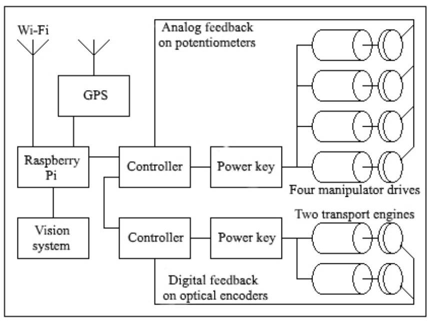

Figure 4. Functional diagram of the control system

Based on the various purposes of the actuators, different types of feedback were selected. For two travel degrees of freedom, the feedback on optical encoders is used; it allows for the odometric navigation in addition to GPS to improve motion accuracy. For four manipulator drives, the feedback with potentiometers is selected.

The control of these actuators is based on two one-type four-channel drive controllers. Each of the controllers is built on two Microchip PIC16F73 microcontrollers with two PWM generators for motor control. The feedback is implemented with four Avago HCTL-2017 microcircuit counters optical quadrature encoders. In this way, each controller provides four complete feedback drive control channels. In addition, each controller has eight GPIO lines (general purpose digital input-output) and five analog input lines; with their help, the feedback of the drives is implemented using a potentiometer instead of optical encoders.

To connect the controllers to the control computer, a proprietary bus is used; it is based on RS-232 but differs electrically and uses an additional protocol [8].

3.2. Sensor system

The sensor system consists of two main components: one is rigidly attached to actuators, and the second, which performs most of the functions of global navigation and spatial orientation, as well as computer vision, is connected to the top-level control unit.

The feedback on the running drives implements odometric navigation, and the feedback of the actuators provides accurate positioning of the manipulator. The global navigation system includes a GPS receiver, the data from which are combined with the readings of odometric sensors on wheels.

3.3. Software architecture

Following the two-level organization of the hardware, the software of the weeding robot includes function libraries for working with lower-level modules and upper-level client programs. The function libraries for working with controllers provide the transmission of control commands and poll of the navigation data and position sensors of the manipulator.

Top-level programs include the following core modules: a navigation system that polls a GPS receiver and combines GPS and odometer data; computer vision system; manipulator control system that implements the algorithms for precise positioning of the operating body; motion control system; top level planning system.

4. Complete model of manipulator dynamics

The generalized coordinates of the manipulator are the lengths of the actuating links $q_1 = l_1, \quad q_2 = l_2, \quad q_3 = l_3,$ and the angles of rotation of the actuating links in relation to the moving coordinate axes $q_4 = \alpha_2, \quad q_5 = \alpha_3$. Three coordinates are independent. Holonomic constraints are superimposed on the coordinates $q_2 = l_2$, $q_3 = l_3$, $q_4 = \alpha_2$, $q_5 = \alpha_3$

$$f_1 = l_2 \cdot \cos\alpha_2 - l_3 \cdot \cos\alpha_3 - AB = 0 \tag{13}$$

$$f_2 = l_2 \cdot \sin\alpha_2 - l_3 \cdot \sin\alpha_3 = 0 \tag{14}$$

Assume that the mechanism for operating body moving consists of seven masses: the mass of the rod of the first actuating link together with the mass of the slider m_1; two actuator cases with the mass m_{21}, m_{31}; two rods with mass m_{22} and m_{32}; mass of the articulated slider m_4 together with the operating body and the mass of the slider m_5.

Since the weeding robot is a multi-mass mechanism, the dynamics of its motions is described by a system of nonlinear differential equations. They are formed using the Lagrange equations with indefinite multipliers and additional holonomic constraints.

$$\frac{d}{dt}\left(\frac{\partial T}{\partial \dot{q}_i}\right) - \frac{\partial T}{\partial q_i} = Q_i + \lambda_1 \frac{df_1}{dq_i} + \lambda_2 \frac{df_2}{dq_i}, \quad i = 1 \div 5 \tag{15}$$

The total kinetic energy T of the manipulator has the form

$$T = T_1 + T_2 + T_3 + T_4 + T_5$$

where T_1 is the kinetic energy of the link 1; T_2 is a total kinetic energy of the link 2; T_3 is a total kinetic energy of the link 2; T_4 is the kinetic energy of the link 4; T_5 is the kinetic energy of the link 5.

The first link of the mechanism performs a rectilinear translational motion. The bodies of the second and third actuators make complex motions: transient translational and relative rotational around a fixed axis. The rods of these actuators also make complex motions: transient translational and relative plane-parallel. The motion of the articulated slider with the mass m_4 consists of the sum of the translation motions, and the slider with mass m_5 performs translational motion.

Using the expressions of kinetic energy and the equations of holonomic constraints (13, 14), obtain five differential equations describing the weeding robot mechanism dynamics [9]

Under the known laws of motion of the operating body of the manipulator, from the expressions the driving forces $F_i(t),\ i = 1 \div 3$ are obtained providing for the execution of the programmed motion; in addition, the values of dynamic loads in kinematic pairs are defined.

5. A numerical example of a control algorithm implementation

Initially, the operating body of the manipulator was at the point with coordinates $x_{40} = 60$ mm, $y_{40} = 300$ mm. The distance between the axes of the attachment points of the actuators $AC = BC = 140$ mm. The lengths of the actuating links $l_{10} = 0$ mm, $l_{20} = 360$ mm, $l_{30} = 310$ mm correspond to these coordinates. Having set the coordinates of the end point $x_4 = -120$ mm, $y_4 = 420$ mm and applying the positioning algorithm, obtain $l_1^{op} = 93{,}5$ mm, $l_2^{op} = 327$ mm, $l_3^{op} = 417{,}4$ mm.

Figures 5 and 6 show the results of computations when moving the operating body from a position defined by the coordinates $x_{40} = 60$ mm, $y_{40} = 300$ mm to a point with coordinates $x_4 = -120$ mm, $y_4 = 420$ mm according to the laws (10): initial velocity $\dot{l}_{i0} = 0$;

$$l_i(t) = l_i^{op} + \frac{\Delta l_{i0}}{p_{1i} - p_{2i}}\left(p_{2i}e^{p_{1i}t} - p_{1i}e^{p_{2i}t}\right),\ \Delta l_i(t) = l_i^{op} - l_{i0},\ p_{1i} = -12,\ p_{2i} = -20$$

$$\Delta l_{10} = 93{,}5 \text{ mm},\ \Delta l_{20} = -33 \text{ mm},\ \Delta l_{30} = 107{,}4 \text{ mm}.$$

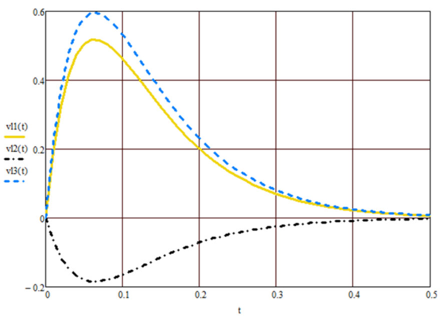

Figure 5. The laws of change in actuator speed

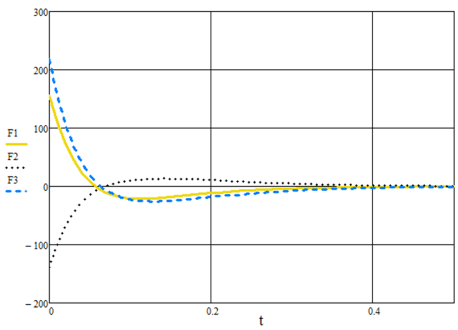

Figure 6. Laws of change of programmed forces of actuator drives

From the graphs (Figure 5, 6) it is seen that during $\tau = 0.5s$ the grip is stabilized in a given position. The deviations from the set position do not exceed 0.1%, and the speeds and accelerations are practically equal to zero. The point path slightly differs from a straight line. If the generalized coordinates of the manipulator deviate from the program path, it makes no sense to stabilize them on the original program path, since for each current point another program path is constructed that satisfies the same final conditions [10]. Figure 6 presents the laws of change in driving forces obtained as a result of solving the equations (16-20).

Conclusion

The problem of positioning the manipulator and the problem of weak terminal control are solved. The program path is corrected in such a way that at any specific time it passes through the current position of the operating body. Over time, the operating body gets into the final region of the target point. An algorithm for generating control voltages is formed taking into account the kinematic parameters of the manipulator in all degrees of freedom. Mathematical modeling showed that the proposed algorithm allows the manipulator grip motion along the program path with an error not exceeding 1%. The algorithm also functions properly in the presence of initial disturbances.

Acknowledgments

The reported study was funded by RFBR according to the research project №19-31-50031

References

1. A. S. Ovchinnikov, V. S. Bocharnikov, N. S. Vorob`eva, A. V. Dyashkin, A. G. Ivanov, I. A. Nesmiyanov, V. V. Zhoga and V. V. Dyashkin-Titov 2019 Pat. 2694588 Russian Federation, MPK A01V 39/18. Robotic weeding with the function of fertigation Byul. № **20**.
2. V.V. Bushuev, I.G. Hol'shev The mechanisms of parallel structure in mechanical engineering. STIN. No.**1**, pp. 3-8 (2001)
3. M.Z. Kolovskii, A.V. Sloushch Foundations of Industrial Robot Dynamics, (M: Nauka). p. 240 (1998)
4. V.V. Kozlov, V.P. Makary`chev, A.V. Timofeev, E.I. Yurevich The dynamics of robot control, (M: Nauka). p.336 (1984)
5. Banday Brian D. Basic Optimisation Methods. Edward Arnold (Publishers) Limited, London WCIB 3DQ
6. A.I. Korendesev, B.L. Salamandra, L.I. Tyves Theoretical Foundations of Robotics: in 2 books. (M: Nauka). Book **1**, p. 383 (2006)
7. P.D. Krut'ko Inverse problems of dynamics of controlled systems: nonlinear models. (M: Nauka). p. 328 (1988)
8. V.E. Pavlovskij, V.V. Pavlovskij Modular microcontroller robot control system ROBOKON-1 // KIAM Preprints M.V. Keldysh. № **86**. pp32. (2012)
9. A. G. Ivanov, V. V. Zhoga, V.E. Pavlovskij and N. S. Vorob`eva Dynamic model of end-effector actuator used for mobile robotic weeder, *IOP Conference Series,* Vol. 747(2019)
10. V. Kh. Pshikhopov, Analytical design of nonlinear terminal control systems, pp. 125-141(1995)